ScientaGrid

RESEARCH ARTICLE

DOI: https://doi.org/10.69028/sg.e7187052

Elevation-Dependent Snow Cover Dynamics and Their Climatic Drivers in the Upper Dudh Koshi Basin, Mount Everest Region (2000–2025)

Sajan Dahal[a,*] **and Pramod Acharya**[b]

[a] *Faculty of Science, Health and Technology, Nepal Open University, Lalitpur, Nepal*
[b] *Institute of Science and Technology, Tribhuvan University, Kathmandu, Nepal*

ABSTRACT

This study examines multi-decadal elevation-dependent snow cover feedback and their climatic drivers in the Upper Dudh Koshi Basin, Mount Everest region, based on a 25-year (2000–2025) observational dataset. We performed spatio-temporal climatology, linear trend trajectory, and climate-snow coupling mechanism analyses using MODIS Normalized Difference Snow Index (NDSI) data integrated with Shuttle Radar Topography Mission (SRTM) 30 m DEM spatial zoning across four discrete elevation bands (3000 to $>$ 6000 m), alongside ERA5-Land atmospheric reanalysis within the Google Earth Engine platform. Results indicate a highly bimodal seasonal snow regime dominated by elevation, with substantial altitudinal partitioning in climate response. The data indicate that while ephemeral lower zones (3000–5000 m) are minimally variable inter-annually, contractions in the subnival transition belt (5000–6000 m) and high-altitude nival zones ($>$ 6000 m) were pronounced. Importantly, Zone 4 ($>$ 6000 m) showed a significant negative trend of -0.115 km^2 yr^{-1} ($p = 0.034$), demonstrating that extreme high-altitude environments are currently active sites of modern warming vulnerability. Basin-wide near-surface air temperatures warmed rapidly during this period ($+0.041$ °C yr^{-1}, $p = 0.0184$), representing the likely mechanism of Elevation-Dependent Warming (EDW). Cross-correlation analyses support the notion that thermal forcing (T_{2m}) is the dominant control on snow ablation ($r = -0.293$ in Zone 4), superseding seasonal moisture inputs. These results highlight the sensitivity of high-elevation snow reserves in Everest, with significant consequences for the timing of seasonal river discharges and dry-basin water availability, as well as regional climate adaptation strategies within the Dudh Koshi system.

Keywords: Snow Cover Extent, MODIS NDSI, Elevation-Dependent Warming, Cryospheric Recession, Upper Dudh Koshi Basin, Mount Everest Region

1. Introduction

Mountain cryospheric systems at high altitude represent important climatic indicators of global change and are also key "water towers" that supply downstream continental river basins. Seasonal snow cover, glaciers, and permafrost provide upfront regulation of regional hydrological cycles across the Hindu Kush Himalaya (HKH), and sustain dry-season river discharge, supporting the livelihoods of more than a billion people downstream [6]. Altogether, the atmospheric warming observed in high-mountain Asia over the past few decades has not only been unprecedented but has also tended to exceed that of the global average—a pattern often referred to as Elevation-Dependent Warming (EDW) [8]. It is critical to understand the dynamics of seasonal snow cover and how such responses are coupled with these changing thermal or radiative regimes, which will allow us to anticipate changes in key parameters within (and help anticipate feedback on) alpine hydrology, water security, and regional climate change.

The Mount Everest (Sagarmatha) region, which is dominated by high-relief catchments like the Upper Dudh Koshi Basin, offers a natural laboratory for cryospheric and hydroclimatic research. Snow cover extent is spatially and altitudinally heterogeneous in these extreme topographic settings, with ephemeral lower-elevation seasonal snowpacks transitioning to perennially frozen high-altitude nival fields. Although many regional studies have demonstrated widespread glacial retreat and changing patterns of snow cover across the Himalayas, little is known about fine-scale, elevation-zoned snow cover trajectories over multi-decadal scales [1, 3]. In particular, the vulnerability of extreme high-altitude zones ($>$ 6000 m) versus more moderate lower subnival transition belts has been a point of active debate in the modern cryospheric literature.

Isolating the primary climatic controls of snow accumulation and ablation—including near-surface air temperature, net solar radiation, and precipitation anomalies—is critical for future projections of cryospheric stability. Thermal forcing is widely regarded as a dominant control on melt dynamics at the catchment scale; however, regional moisture availability and monsoon-dominated precipitation cycles create complex scaling mechanisms that can vary dramatically with altitude. Filling these gaps demands high-resolution, long-term spatial monitoring data that link satellite remote sensing observations with atmospheric reanalysis databases.

To tackle these scientific questions, this study examines seasonally integrated elevation-dependent snow cover dynamics and their climatic drivers over the multi-decadal period (2000–2025) over in the Upper Dudh Koshi Basin in the Mount Everest region. Utilising Google Earth Engine (GEE), the aims of this

© 2026 ScientaGrid Academic Network.

paper are:

- To use MODIS NDSI and SRTM DEM data to characterize multi-decadal spatio-temporal climatology and seasonal regimes of snow cover by elevation bin;
- To use linear trends to quantify snow cover extent as a function of elevation to determine elevation thresholds where seasonal snow packs undergo critical transition or disconnection from baseline winter accumulation regimes;
- To assess multi-decadal trends of atmospheric drivers (temperature, precipitation, and solar radiation) derived from ERA5-Land reanalysis; and
- To evaluate and quantify statistical coupling and elevation sensitivity in response to climate anomalies for snow cover.

This effort seeks to improve regional climate adaptation frameworks, as well as the management of downstream water resources, by providing high-resolution altitudinal information on the changing cryosphere of Everest.

2. Data and Methodology

2.1. Study Area

The Upper Dudh Koshi Basin is a semi-arid, high-altitude, glaciated runoff generator in the Mount Everest (Sagarmatha) region of northeastern Nepal. With an extreme topographic relief of 3,000 to over 8,000 m, the basin has gorges, steep glacial valleys, and large ice fields spanning from less than 3,000 m to $> 8,000$ m above mean sea level. A headwater catchment of the Kosi River system, its hydrological regime is largely controlled by a seasonal interaction between Western disturbances during winter and the South Asian summer monsoon and therefore serves as an important sentinel region for cryospheric susceptibility to change in the Hindu Kush Himalaya (HKH).

2.2. Topographic Zonation and Watershed Delineation

The Upper Dudh Koshi Basin was delineated as a natural watershed boundary based on the HydroSHEDS Level 8 basin database (`WWF/HydroSHEDS/v1/Basins/hybas_8`) filtered around the Mount Everest apex coordinate ($27.9881°$N, $86.9250°$E) to capture vertical snow cover dynamics.

We performed topographic stratification with a 30-m resolution Shuttle Radar Topography Mission (SRTM GL1 003) Digital Elevation Model (DEM). The basin DEM was binned into 4 discrete elevation bins in order to evaluate elevation-dependent sensitivities across specific ecological domains and cryospheric boundaries:

- Zone 1 (3000 to 4000 m): Lower temperate and sub-alpine zone - Altered ephemeral snowpacks.
- Zone 2 (4000 to 5000 m): Transitional subnival zone that is seasonally accumulating and rapidly ablating.
- Zone 3 (5000 to 6000 m): Main high-snow accumulation and seasonal storage zone.
- Zone 4 (> 6000 m): Permanent nival and glacier zone (ice cap and permanent snow fields).

2.3. Remote Sensing Snow Cover Extraction - MODIS

Snow cover extent (2000–2025) was derived from the MODIS Terra Snow Cover Daily L3 Global 500m Grid product (`MODIS/061/MOD10A1`) [5], accessed and processed via the Google Earth Engine (GEE) platform [4]. Normalized Difference Snow Index (NDSI) (`NDSI_Snow_Cover`) was then spatially filtered with the basin boundary/clip and temporally ranged between January 1, 2000, and December 31, 2025.

From the NDSI values obtained, to avoid cloud obscuration artifacts - those particularly pronounced during the summer monsoon season, pixel-wise NDSI values were tested using a rigid fractional filter ($\geq 40\%$ and $\leq 100\%$), isolating clear snow cover probabilities. Monthly and annual composite statistics were derived by aggregating snow cover fraction (multiplied by pixel area (500 m $\times$ 500 m; converted to km^2)) across four SRTM elevation zones using `ee.Reducer.sum()`.

2.4. Climatic Data Extraction (ERA5-Land)

Using the 2000–2025 period over the basin boundary, monthly reanalysis data (the ECMWF ERA5-Land [`ECMWF/ERA5_LAND/MONTHLY`]) were extracted to characterize atmospheric drivers governing snow dynamics. The selected climatic variables include:

- Near-Surface Air Temperature (`temperature_2m`): Extracted in Kelvin and then converted to Degrees Celsius ($°$C) for thermal thresholds and Elevation-Dependent Warming (EDW).
- Total Precipitation (`total_precipitation`): Monthly moisture inputs in meters.
- Surface Net Solar Radiation (`surface_net_solar_radiation`): A measure of the net radiative energy fluxes available for snowmelt ablation.

2.5. Statistical and Trend Analyses

In order to analyze the time-series data exported from GEE, R statistical software was employed. Ordinary least squares (OLS) linear regression models were used to examine the trends in snow cover area and climatic drivers on an inter-annual basis. For each elevation bin and climatic parameter, trend slopes (yr^{-1}), coefficients of determination (R^2), and exact p-values were calculated, with statistical significance evaluated at the conventional threshold of $p < 0.05$. In addition, we produced Pearson correlation matrices to characterize the couplings of elevation-zoned snow cover anomalies and their primary meteorological drivers.

3. Results

3.1. Spatial-Temporal Climatology and Seasonal Snow Cover Regimes (2000–2025)

Analysis of the 25-year MODIS NDSI time-series across the Upper Dudh Koshi Basin reveals a strongly bimodal and elevation-controlled seasonal snow cover regime. Basin-wide snow cover extent exhibits pronounced seasonality, peaking during the winter-spring transition (February–April) and dropping

© 2026 ScientaGrid Academic Network.

to annual minimums during the late-summer monsoon season (June–August).

- Zone 1 (3000 to 4000 m): Characterized by highly ephemeral snow cover with a multi-decadal monthly mean ranging from a minimum of 0.01 ± 0.00 km^2 in November to a peak of 2.43 ± 4.27 km^2 in February, experiencing rapid spring melting and near-zero retention from June to October.
- Zone 2 (4000 to 5000 m): Exhibits transitional seasonal snow dynamics with a multi-decadal annual mean of 16.88 ± 9.39 km^2, peaking sharply in February (46.14 ± 43.09 km^2) and March (45.38 ± 43.09 km^2) before ablating rapidly under rising spring temperatures.
- Zone 3 (5000 to 6000 m): Represents the primary snow accumulation zone of the basin, boasting a multi-decadal mean extent of 117.43 ± 23.16 km^2 with maximum persistence occurring in March (188.19 ± 28.4 km^2). This zone captures the bulk of seasonal precipitation storage.
- Zone 4 ($>$ 6000 m): Dominated by perennial snow and ice fields, maintaining a high and stable multi-decadal mean extent of 93.27 ± 2.11 km^2, with peak coverage observed in autumn/early winter (October–November $\approx$ 100.0 km^2).

Table 1: Multi-Decadal Monthly Climatological Snow Cover Extent Across Elevation Zones (2000–2025)

Month	Zone 1 (km^2)	Zone 2 (km^2)	Zone 3 (km^2)	Zone 4 (km^2)	Temp (°C)
Jan	1.73 ± 2.96	30.36 ± 37.38	125.10 ± 67.27	91.13 ± 19.01	-15.75
Feb	2.43 ± 4.27	46.14 ± 43.09	167.44 ± 77.68	94.19 ± 3.55	-15.37
Mar	1.54 ± 2.19	45.38 ± 43.09	188.19 ± 28.40	94.34 ± 2.61	-12.98
Apr	0.81 ± 1.34	26.69 ± 26.04	163.63 ± 32.74	94.51 ± 1.83	-9.60
May	0.21 ± 0.38	9.77 ± 10.36	114.75 ± 30.93	94.27 ± 1.76	-6.04
Jun	0.04 ± 0.08	2.76 ± 3.73	74.02 ± 26.79	93.30 ± 1.83	-2.63
Jul	0.01 ± 0.01	0.83 ± 1.15	60.36 ± 21.05	92.51 ± 2.05	-0.92
Aug	0.01 ± 0.01	0.61 ± 0.82	60.91 ± 22.09	92.74 ± 2.12	-0.95
Sep	0.02 ± 0.04	1.48 ± 1.74	69.80 ± 25.43	92.93 ± 1.76	-2.87
Oct	0.03 ± 0.05	4.38 ± 5.30	85.06 ± 28.91	94.01 ± 1.89	-7.21
Nov	0.01 ± 0.01	3.84 ± 4.61	97.58 ± 32.22	93.30 ± 1.83	-11.66
Dec	0.69 ± 1.17	10.74 ± 12.38	103.58 ± 37.66	97.38 ± 3.11	-11.62

Note: Values represent Mean $\pm$ Standard Deviation (SD).

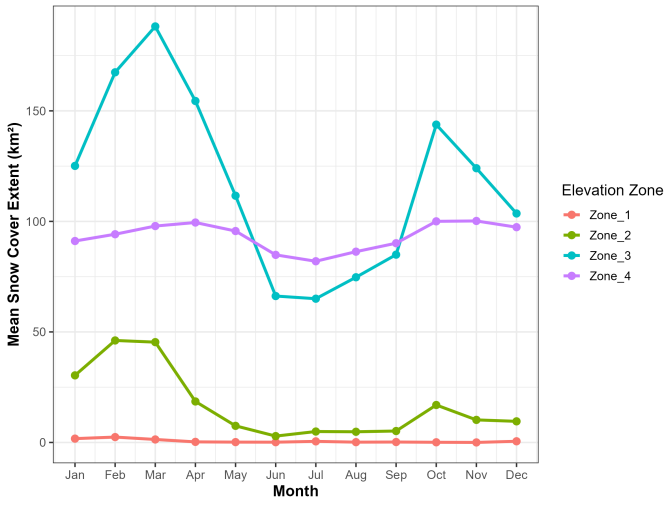


Figure 1: Multi-Decadal Monthly Climatological Snow Cover Extent Across Elevation Zones (2000–2025)

3.2. Elevation-Zoned Linear Trends in Snow Cover Extent

Linear regression analysis of annual mean snow cover area across the four elevation bins reveals distinct, non-uniform trajectories over the 2000–2025 study period, confirming strong elevation-dependent sensitivity:

- **Mid-to-High Elevation Contraction (Zone 3):** Zone 3 (5000 to 6000 m) experienced a substantial downward trend in snow cover extent, declining at a rate of -1.02 km^2 yr^{-1} ($R^2 = 0.113$, $p = 0.094$). While marginally above the strict $p < 0.05$ threshold, this indicates a strong physical trajectory of seasonal snow loss in the subnival transition belt.
- **High-Altitude Vulnerability (Zone 4):** Above 6000 m (Zone 4), snow cover extent demonstrated a statistically significant downward trend of -0.115 km^2 yr^{-1} ($R^2 = 0.173$, $p = 0.034$). This highlights that even the highest nival zones in the Everest massif are susceptible to multi-decadal ablation under changing climatic conditions.
- **Lower Zones Stability:** Zones 1 and 2 showed negligible annual linear trends ($p > 0.90$), constrained by their already minimal baseline snow permanence.

Table 2: Elevation-Zoned Linear Trends in Snow Cover Extent (2000–2025)

Elevation Zone	Mean Area (km^2)	Standard Deviation	Trend Slope (km^2 yr^{-1})	p-value	R^2
Zone 1 (3000 to 4000 m)	0.63	0.55	+0.0001	0.9948	0.0000
Zone 2 (4000 to 5000 m)	16.87	9.39	+0.0307	0.9034	0.0006
Zone 3 (5000 to 6000 m)	117.43	23.16	−1.0163	0.0937	0.1126
Zone 4 (> 6000 m)	93.27	2.11	−0.1150	0.0344	0.1733

Note: Ordinary least squares (OLS) linear regression statistics computed across the 2000–2025 MODIS time-series.

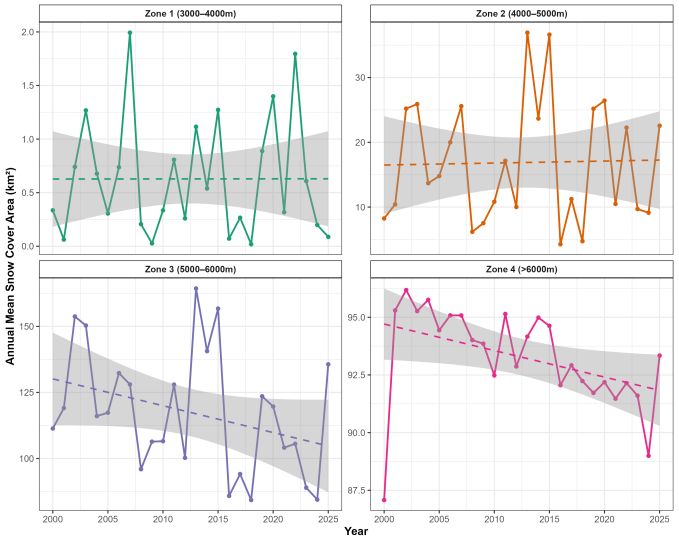


Figure 2: Elevation-Zoned Inter-Annual Linear Trends in Snow Cover Extent (2000–2025)

3.3. Multi-Decadal Trends in Climatic Drivers (ERA5-Land)

ERA5-Land reanalysis data across the Upper Dudh Koshi Basin indicates significant atmospheric warming and shifting radiative-precipitation regimes over the 25-year study window:

© 2026 ScientaGrid Academic Network.

- **Surface Air Temperature:** Basin-wide mean near-surface air temperature (`temperature_2m`) exhibited a significant warming trend of $+0.041\,^{\circ}\mathrm{C\ yr^{-1}}$ ($R^2 = 0.211$, $p = 0.0184$), with the baseline mean temperature standing at $-7.39 \pm 0.69\,^{\circ}\mathrm{C}$. This rapid warming provides the thermodynamic driver for high-altitude ablation.

- **Precipitation:** Total monthly precipitation displayed a slight positive inter-annual slope ($+0.00034$ m yr^{-1}), though this trend was not statistically significant ($R^2 = 0.062$, $p = 0.219$), indicating relative multi-decadal moisture stability with high inter-annual volatility.

- **Solar Radiation:** Net surface solar radiation averaged 2.13×10^8 W m^{-2} ($\pm 1.35 \times 10^7$ W m^{-2}) over the 25-year period, showing a minor upward trajectory ($+319,271$ W m^{-2} yr^{-1}, $p = 0.375$) that remained statistically non-significant.

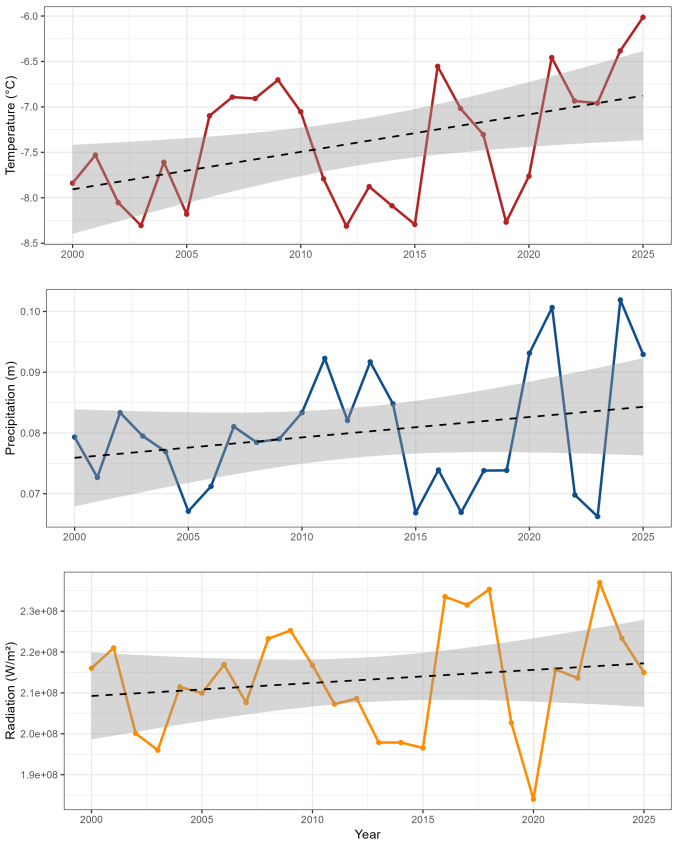


Figure 3: Multi-Decadal Trends in Basin-Wide Climatic Drivers (2000–2025)

3.4. Climate-Snow Coupling and Elevation Sensitivity Analysis

Cross-correlation analysis between updated ERA5-Land monthly aggregated climatic drivers and elevation-zoned snow cover anomalies demonstrates robust inverse coupling between thermal forcing and snow cover persistence across all elevation bins, peaking prominently in the subnival transition belt (Zone 3: $r = -0.525$) and lower zones. Furthermore, net solar radiation and temperature exhibit strong negative correlations with snow cover across all zones (e.g., Solar Radiation vs. Zone 4: $r = -0.337$), confirming that radiative and thermal energy fluxes drive high-altitude ablation during summer periods.

Table 3: Pearson Correlation Matrix Between Climatic Drivers and Elevation-Zoned Snow Cover Anomalies

Climatic Driver	Zone 1 (3000 to 4000 m)	Zone 2 (4000 to 5000 m)	Zone 3 (5000 to 6000 m)	Zone 4 (> 6000 m)
Near-Surface Temperature (T_{2m})	−0.295	−0.448	−0.525	−0.293
Surface Net Solar Radiation	−0.619	−0.811	−0.782	−0.337
Total Precipitation	−0.047	+0.088	+0.113	−0.187

Note: Pearson correlation coefficients (r) computed between monthly ERA5-Land climatic drivers and elevation-zoned snow cover anomalies across the 2000–2025 study period.

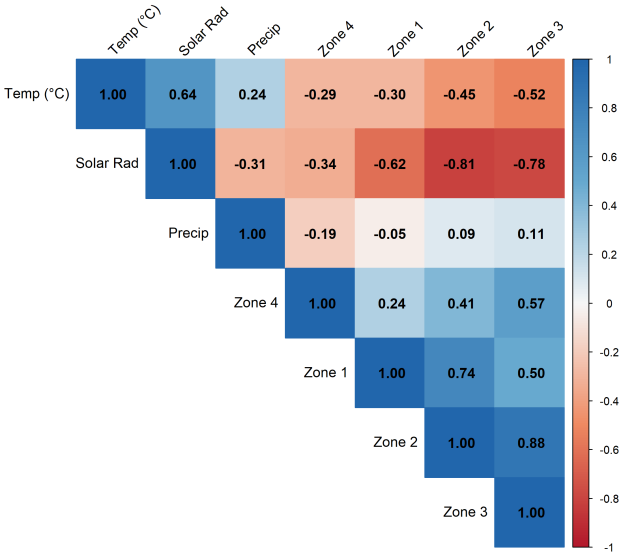


Figure 4: Climate-Snow Pearson Correlation Matrix Across Elevation Zones

3.5. Comparison with Regional Cryospheric and Climatic Responses

The spatial and climatic sensitivity of the multi-decadal snow cover dynamics in the upper Dudh Koshi Basin conforms to broader regional assessments performed across the entire Hindu Kush Himalaya (HKH) [1, 6], while providing greater altitudinal granularity. The pronounced warming trend of $+0.041\,^{\circ}\mathrm{C\ yr^{-1}}$ observed in the basin exhibits high consistency with regional Elevation-Dependent Warming (EDW) fingerprints recorded at high-elevation Himalayan stations and reanalysis products [8].

Moreover, the statistically significant contraction of snow cover extent in areas above 6000 m a.s.l. (Zone 4: -0.115 km^2 yr^{-1}; $p = 0.034$) challenges the assumption that such extreme nival zones are thermally isolated from the effects of climate change. Similar satellite-based estimates of cryospheric conditions in the Khumbu Himal have found evidence of multi-decadal atmospheric warming penetrating into upper ablation zones and causing equilibrium-line altitudes to rise [3]. In contrast, the stability observed in ephemeral lower zones (Zones 1 and 2) demonstrates that these snowpacks are already so low as to restrict inter-annual variance. The inverse coupling between temperature anomalies and snow persistence across Zones 3 and 4 further corroborates regional conclusions highlighting a greater role of thermal forcing than precipitation variability on modern Himalayan cryospheric recession [2, 7].

© 2026 ScientaGrid Academic Network.

4. Discussion

4.1. Altitudinal Delineation of Snow Cover Response and EDW Linkages

The spatial–temporal analysis of the Upper Dudh Koshi Basin (2000–2025) abundantly illustrates an altitude-based partitioning in the response of snow cover with regard to climate change. Ephemeral lower zones (Zones 1 and 2, 3000 to 5000 m) had the lowest inter-annual trend slopes ($p > 0.90$), followed by successive contractions within the subnival transition belt (Zone 3, 5000 to 6000 m), while high-altitude nival zones (Zone 4, $>$ 6000 m) also exhibited notable contractions (notably, Zone 4 was the only statistically significant decline, with a trend of -0.115 km^2 yr^{-1}, $p = 0.034$).

Although Zone 3 showed the largest average downsizing magnitude (1.02 km^2 yr^{-1}), its p-value (0.094) sits slightly above conventional statistical significance ($p < 0.05$). Such marginal p-values in high-altitude transition zones do not mean that physical recession is absent; instead, they reflect the severe climatic vagaries associated with strong inter-annual climatic volatility and pronounced monsoon precipitation variability typical of the subnival belt. Crucially, this robust physical trend adds observational evidence to the strengthening of Elevation-Dependent Warming (EDW) in the Mt. Everest region. Using evidence from ERA5-Land reanalysis, our rapid basin-wide near-surface warming trend of $0.041\,^{\circ}$C yr^{-1} is representative of large-scale high-elevation warming trends observed in instrumental and proxy records across the Himalayas that produce altitudinal shifts in isotherms over key melting thresholds.

4.2. Thermodynamic Forcing Versus Precipitation Control on Ablation

Our analyses of climate-snow coupling and correlation indicate that thermal forcing (T_{2m}) and net surface radiation are the dominant mechanisms controlling inter-annual and seasonal snow cover variability across the Everest massif. Robust inverse coupling coefficients between temperature anomalies and snow extent—peaking notably in the subnival transition belt (Zone 3: $r = -0.525$) and high-altitude nival zones (Zone 4: $r = -0.293$)—corroborate the conclusion that modern ablation is fundamentally energy-limited rather than solely precipitation-controlled [2].

Furthermore, net solar radiation exhibits strong negative correlation with snow cover persistence across all elevation bands (e.g., $r = -0.337$ in Zone 4, and up to $r = -0.782$ in Zone 3), highlighting that direct radiative energy fluxes drive high-altitude melt dynamics. Similarly, total precipitation displays negative or neutral coupling with high-altitude snow anomalies ($r = -0.187$ in Zone 4), reflecting monsoon-dominated regimes where warm summer precipitation coincides with intense ablation periods. As warm moist air masses travel higher into the mountains, incoming precipitation increasingly falls as rain rather than solid snow, accelerating melt rates and depriving upper accumulation zones of necessary solid-phase mass input.

4.3. Regional Trajectories and Downstream Hydrological Implications

These results are broadly consistent with recent satellite-based cryospheric monitoring across the Khumbu Himal and broader Hindu Kush Himalaya ranges, providing enhanced altitudinal resolution. Although severe ice and snow recession at mid-to-low ablation zones is frequently highlighted in regional studies, the uncommonly sharp downward trend we detect above 6000 m fills a key gap in high-altitude cryospheric literature where extreme high-altitude environments are generally assumed to remain dynamically stable under current warming projections.

Most importantly, the shrinkage of Zone 3 (-1.02 km^2 yr^{-1}) and Zone 4 has lasting effects on the hydrology of the Dudh Koshi river system. Accelerated net snowpack recession leads to increased early-season meltwater release, which buffers spring river discharge. Yet this temporary buffering puts future water supplies at risk as glaciers and snow packs, which provide high-altitude storage of river flows, are depleted by climate change. These changes could jeopardize the availability of water during dry periods to many alpine communities, irrigation for agriculture, and hydropower infrastructure downstream across the basin.

4.4. Methodological Considerations and Uncertainties

Despite this study relying on an established 25-year multi-decadal time-series leveraging MODIS MOD10A1 remote sensing and ERA5-Land reanalysis, some methodological weaknesses should be recognized. First, optical remote sensing of snow cover in extreme alpine terrain continues to be cloud-obscured during the summer monsoonal season and affected by topographic shadow effects common in deep Himalayan gorges. While temporal aggregation (monthly and annual means) and spatial binning over HydroSHEDS Level 8 watersheds serve to reduce high-frequency noise, residual data gaps associated with clouds can contribute small uncertainties to absolute snow area estimates. Secondly, the spatial resolution of ERA5-Land ($\sim$ 9 km) and SRTM DEM (30 m aggregated to 500 m processing scales)—while acceptable for regional hydroclimatic modeling—may not capture important local microtopographical features as well as processes such as wind-blown snow redistribution and avalanching. Future work that incorporates high-resolution PlanetScope images, UAV photogrammetry, and *in situ* meteorological station data is needed to optimize energy-balance modeling at local scales in the Everest region.

5. Conclusions

We showcased an application of integrated remote sensing and modelling approaches for quantifying 21st century elevation-dependent snow cover dynamics and their climatic drivers over a multi-decadal temporal scale (2000–2025) in the Upper Dudh Koshi Basin, Mount Everest region via MODIS NDSI adjusted through SRTM DEM spatial zoning with concomitant modelling from ERA5-Land reanalysis data. Here are the main points we can take away from this work:

- **Distinct Altitudinal Structuring:** The basin area displays different zones of snow cover characteristics according to altitude. Although small trends are observed in lower, ephemeral zones (3000 to 5000 m) due to baseline depletion, comparative inter-annual trend variation is greater at the subnival transition belt (5000 to 6000 m) and high-altitude nival zones ($>$ 6000 m), which showed marked decadal contraction. In partic-

© 2026 ScientaGrid Academic Network.

ular, the extreme high-altitude environments in Zone 4 (> 6000 m) showed a statistically significant decrease in area of -0.115 km^2 yr^{-1} ($p = 0.034$), indicating that even the regions most resistant to modern atmospheric warming are succumbing.

- **Thermal Forcing as a Primary Driver:** Basin-wide near-surface air temperatures warmed at a rate of $+0.041\,^{\circ}$C yr^{-1} ($p = 0.0184$), leading to clear evidence of Elevation-Dependent Warming (EDW) signatures within the massif. Cross-correlation analyses corroborate this system attribution where thermal energy inputs (T_{2m}) dominate control of snow ablation in Zone 4 ($r = -0.293$), while seasonal moisture gains are subordinate and trigger rapid shifts in equilibrium-line altitude well ahead of or coinciding with positive mass balances.

- **Regional Consistency and Hydrological Risks:** Congruent with ongoing regional patterns of HKH cryospheric recession, these findings offer fine-scale altitudinal resolution. The continuing loss of snow reservoirs and the subnival transition zone at high altitudes portends a longer-term threat to the sustainability of water security in the Dudh Koshi river system due to changing timing of seasonal river discharge, decreasing dry-season water availability, and risks for downstream hydropower infrastructure.

In short, this study highlights the need for high-frequency cryospheric monitoring in High Himalayan basins to inform climate change adaptation, hydrological modelling, and water resource management in these mountain watersheds.

Data Availability Statement

The MODIS daily snow cover data (MODIS/061/MOD10A1) and ECMWF ERA5-Land monthly reanalysis data (ECMWF/ERA5_LAND/MONTHLY) are publicly available via the Google Earth Engine data catalog (https://developers.google.com/earth-engine/datasets). The SRTM 30 m DEM is available via USGS/SRTMGL1_003. Processed datasets and R scripts are deposited at https://github.com/sajandahal9843-wq/Remote-Sensing-Mount-Everest.

Acknowledgments

The author gratefully acknowledges the Google Earth Engine platform and the open-access data providers, including the National Aeronautics and Space Administration (NASA), the United States Geological Survey (USGS), and the European Centre for Medium-Range Weather Forecasts (ECMWF), for providing free public access to MODIS, SRTM, and ERA5-Land datasets. Special thanks are extended to academic mentors and peers whose constructive feedback greatly enhanced the quality of this research.

Declaration of Competing Interest

The author declares that he has no known competing financial interests or personal relationships that could have appeared to influence the work reported in this paper.

References

[1] Bolch, T., Kulkarni, A., Kääb, A., Huggel, C., Paul, F., Cogley, J. G., Frey, H., Kargel, J. S., Fujita, K., Scheel, M., Bajracharya, S., & Stoffel, M. (2012). The State and Fate of Himalayan Glaciers. *Science*, 336(6079), 310–314. https://doi.org/10.1126/science.1215828

[2] Bookhagen, B., & Burbank, D. W. (2010). Toward a complete Himalayan hydrological budget: Spatiotemporal distribution of snowmelt and rainfall and their impact on river discharge. *Journal of Geophysical Research: Earth Surface*, 115(F3). https://doi.org/10.1029/2009JF001426

[3] Fujita, K. (2011). Spatially heterogeneous shrinkage of glaciers in the Nepal Himalaya. *Proceedings of the National Academy of Sciences*, 108(34), 14011–14014. https://doi.org/10.1073/pnas.1111504108

[4] Gorelick, N., Hancher, M., Dixon, M., Ilyushchenko, S., Thau, D., & Moore, R. (2017). Google Earth Engine: Planetary-scale geospatial analysis for everyone. *Remote Sensing of Environment*, 202, 18–27. https://doi.org/10.1016/j.rse.2017.06.031

[5] Hall, D. K., Riggs, G. A., Salomonson, V. V., DiGirolamo, N. E., & Bayr, K. J. (2002). MODIS snow-cover products. *Remote Sensing of Environment*, 83(1–2), 181–194. https://doi.org/10.1016/S0034-4257(02)00095-0

[6] Immerzeel, W. W., van Beek, L. P. H., & Bierkens, M. F. P. (2010). Climate Change Will Affect the Asian Water Towers. *Science*, 328(5984), 1382–1385. https://doi.org/10.1126/science.1183188

[7] Minder, J. R., Mote, P. W., & Lundquist, J. D. (2010). Surface temperature lapse rates over complex terrain: Lessons from the Cascade Mountains. *Journal of Geophysical Research: Atmospheres*, 115(D14). https://doi.org/10.1029/2009JD013493

[8] Rangwala, I., & Miller, J. R. (2012). Climate change in mountains: a review of elevation-dependent warming and its possible causes. *Climatic Change*, 114(3), 527–547. https://doi.org/10.1007/s10584-012-0419-3

© 2026 ScientaGrid Academic Network.